Bioinformatics, YYYY, 0–0
doi: 10.1093/bioinformatics/xxxxx
Advance Access Publication Date: DD Month YYYY
Discovery Notes

Gene expression

Systematic determination of the mitochondrial proportion in human and mice tissues for single-cell RNA sequencing data quality control

Daniel Osorio[1, *], and James Cai[1, 2, 3]

1 Department of Veterinary Integrative Biosciences, 2 Department of Electrical & Computer Engineering, and 3 Interdisciplinary Program of Genetics, Texas A&M University, College Station, TX 77843-4458, USA

*To whom correspondence should be addressed.

Associate Editor: XXXXXXX

Received on XXXXX; revised on XXXXX; accepted on XXXXX

Abstract

Motivation: Quality control (QC) is a critical step in single-cell RNA-seq (scRNA-seq) data analysis. Data from low-quality cells is removed during the QC process in order to yield genuine, biologically meaningful results. One of the important QC metrics is the mitochondrial proportion (mtDNA%), i.e., the fraction of mitochondrial transcript counts of the total transcript counts. The mtDNA% threshold is used to filter out apoptotic, stressed, low-quality cells in the data. Early publications in the field established a threshold of 5% and since then, it has been used as a default parameter in several software packages for scRNA-seq data analysis. Furthermore, such a single threshold of mtDNA% has been adapted as a standard and used in many scRNA-seq studies. However, the validity of using such a uniform threshold across different species, single-cell technologies, tissues, and cell types has not been adequately assessed.

Results: We systematically analyzed 5,530,106 cells reported in 1,349 annotated datasets available in the PanglaoDB database and found that the average mtDNA% in scRNA-seq data across human tissues is significantly higher than that across mouse tissues. This difference is not confounded by single-cell platforms and technologies used to generate the data. Based on this finding, we propose new reference values of the mtDNA% threshold for 121 tissues of mouse and 44 tissues of humans. In general, for mouse tissues, with very few exceptions (3 of 121 analyzed tissues), the 5% threshold can still be used as a default, which performs well to distinguish between healthy and low-quality cells. For human tissues, the 5% threshold should be reconsidered as it fails to accurately discriminate between healthy and low-quality cells in 29.5% (13 of 44) tissues analyzed.

Availability: The code used to download datasets, perform the analyzes, and produce the figures is available at https://github.com/dosorio/mtProportion

Contact: dcosorioh@tamu.edu

Supplementary information: Supplementary data are available at *Bioinformatics* online.

1 Introduction

Single-cell RNA-seq (scRNA-seq) experiments have improved the resolution of our knowledge about cellular composition and cellular behavior in complex tissues (Sandberg 2014). A critical step during scRNA-seq data processing is to perform quality control (QC) over the cells sequenced transcriptomes (Hwang et al. 2018). The QC process usually involves applying user-defined thresholds for different metrics computed for each individual cell to filter out doublets and "low-quality" cells (Luecken and Theis 2019). Commonly used QC metrics include the total transcript counts (also known as the library size), the number of expressed genes, and the mitochondrial proportion (mtDNA%, i.e., the ratio of reads mapped to mitochondrial DNA-encoded genes to the total number of reads mapped). Defining the proper thresholds of QC metrics is a complex task that requires a vast knowledge of the cellular diversity in the tissue under

study. Thresholds may be uniquely set for each sample, as they are dependent on the cells or tissue being processed (Ji and Sadreyev 2019).

Our present study focuses on the systematic determination of a threshold for mtDNA%—the fraction of mitochondrial counts per cell— in scRNA-seq QC. Mitochondrial content is known to interact with the nuclear genome, drive alternative splicing, and regulate nuclear gene expression, and is also associated with cancer, degenerative diseases, and aging (Guantes et al. 2015; Muir et al. 2016). High numbers of mitochondrial transcripts are indicators of cell stress, and therefore mtDNA% is a measurement associated with apoptotic, stressed, low-quality cells (Zhao et al. 2002; Ilicic et al. 2016; Lun et al. 2016). However, mtDNA% threshold depends highly on the tissue type and the questions being investigated (AlJanahi et al. 2018). The mtDNA% threshold is of economic and biological importance. A wrongly defined, very stringent mtDNA% threshold may cause bias in the recovered cellular composition of the tissue under study. This bias may force the researchers to increase the sample size to capture enough cells (which may not have the normal biological behavior of the cell type) under the threshold, and thus increase the cost of the experiment. Inversely, a relaxed threshold of mtDNA% may allow apoptotic, low-quality cells to remain in the analysis, resulting in the identification of wrong biological patterns.

To reduce the bias caused by the use of arbitrary mtDNA% thresholds, Ma and collaborators (Ma et al. 2019) proposed an unsupervised method to optimize the threshold for each given input data. This computationally expensive data driven procedure, which defines the threshold as a function of the distribution of the data, due to the lack of reference values is not able to identify bias induced during the library preparation. Without such standard references, the values of mtDNA% thresholds fluctuate with different input data sets. For example, a largely failed experiment may generate a data set, in which most cells have an inflated mtDNA%. Accordingly, the optimized threshold based on these inflated values may be unreasonably high. Therefore, having a uniform and standardized threshold for scRNA-seq data analysis is essential. It improves the reproducibility of experiments and simplifies the automatization of bioinformatic pipelines (McCarthy et al. 2017).

Through analysis of bulk RNA-seq data produced by the Illumina Body Tissue Atlas, Mercer and collaborators reported the mtDNA% for 16 human tissues (Mercer et al. 2011). They found that the mtDNA% ranges from 5% or less in tissues with low energy requirements up to approximately 30% in the heart due to the high energy demand of cardiomyocytes. Based on that study, early publications of scRNA-seq datasets used the 5% threshold reported for tissues with low energy demands (e.g., adrenal, ovary, thyroid, prostate, testes, lung, lymph, and white blood cells) as default for data quality control (Lukassen et al. 2018). Furthermore, the 5% threshold has been adapted as the default parameter by Seurat—one of the most popular software packages for scRNA-seq data analysis (Satija et al. 2015). These have made 5% a practical standard for scRNA-seq data analyses. Nevertheless, due to the lack of reference values for mtDNA% in different species, technologies, tissues and cell types, the optimal value for a standardized threshold is still an open question in the field.

PanglaoDB is a scRNA-seq database providing uniformly processed, annotated count matrices for thousands of cells from hundreds of scRNA-seq experiments. The data source of PanglaoDB is the sequence read archive (SRA) database of the National Center for Biotechnology Information (NCBI). With the data sets from PanglaoDB, it is possible to systematically evaluate the optimal threshold of mtDNA% for different experimental settings that may vary across platforms, technologies, species, tissues or cell types (Franzen et al. 2019; Svensson et al. 2019). Here, we present a systematic analysis of the mtDNA% in more than 5 million cells reported in over one thousand data sets in PanglaoDB (Franzen et al. 2019). We compared the mtDNA% reported for different technologies, species, tissues, and cell types. By analyzing the data provided by hundreds of experiments together, we reach the consensus reference values for more than 40 human tissues and more than 120 mouse tissues. Furthermore, we evaluated the validity of using the 5% threshold in different tissues in humans and mice.

2 Methods

Datasets in the PanglaoDB database, available at the time of analysis (in January 2020), were downloaded and processed using R 3.6.2 (R Core Team 2013) through an '*in-house*' script using the XML (Lang and CRAN Team 2012) and xml2 (Wickham et al. 2018) packages. The library size (total number of counts), the total number of detected genes, and the total number of counts that match with the mitochondrial genes (mitochondrial counts) were estimated for all cells in each of downloaded datasets. The SRA/SRS identifiers, species, protocol, tissue, cell type and barcode of each experiment were obtained and associated with each cell.

Only the cells with more than $1{,}000$ counts and with the total number of counts greater than two times the average library size in the same sample were retained for analysis. In addition, a polynomic regression of degree 2 (to account for saturation) was applied to establish the 95% confidence intervals of predicted total number of genes as a function of the library size per cell. Cells with an observed total number of genes below or above expectation limits were removed from the analysis. The same procedure was applied a second time to establish the 95% confidence intervals of the predicted mitochondrial counts as a function of library size. An ordinary least squares (OLS) regression model was used to fit the data and cells with exceptionally high or low mitochondrial counts were removed from the analysis.

Subsequently, the mtDNA% value was computed for each cell as the ratio between the mitochondrial counts and the library size of the cell. The mtDNA% values were then compared between cells from different settings: species, technologies, tissues, and cell types. To compare the mtDNA% between humans and mice cells, we used the Welch two-sample *t*-test and used the Wilcoxon sum-rank test to cross validate the results. To evaluate the reliability of the 5% threshold, a comparison to evaluate whether the mean was less than the 0.05 threshold value was performed using the t-test for each tissue and cell type independently using the data generated by the 10X Genomics Chromium system, after filtering out groups with less than $1{,}000$ cells.

3 Results

We downloaded a total of 5,530,106 cells reported in 1,349 datasets from the PanglaoDB database. From those, we removed 278,607 cells with a total number of counts smaller than 1,000 or above two times the average library size in the sample where it was sequenced. Also, 80,225 cells with no mitochondrial counts were removed. The remaining 5,171,274 cells were used to establish the 95% confidence intervals of the predicted total number of genes as a function of the library size per cell (Fig. S1).

We found that the relationship between the number of genes and the library size is monotonically positive ($\rho = 0.89; P < 2.2 \times 10^{-16}$), which is consistent with that previously reported (Svensson, da Veiga Beltrame et al. 2019). We also found that the expected total number of genes reaches saturation at a point close to the 1×10^5 library size counts. In this step, we removed 157,960 cells because they have a total number of quantified genes above ($n = 5{,}509$) or below ($n = 152{,}451$) the 95% confidence interval limit defined from the prediction.

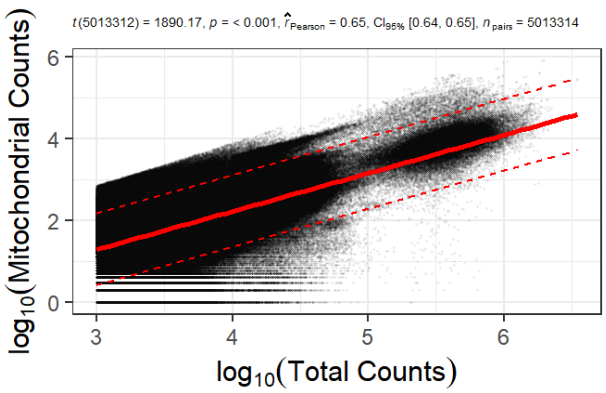

Fig 1. Relationship between the total number of mitochondrial counts and the library size. Each dot represents a cell, the continuous red line represents the expectation and the dotted lines the lower and upper limit of the confidence interval of the prediction computed using OLS regression.

Next, we accounted for outliers in the mitochondrial counts in relative to the library size. This procedure has been shown to be critical to differentiate apoptotic cells of pre-apoptotic and healthy cells in a supervised experiment (Ordonez-Rueda et al. 2020). To do so, we used the OLS regression and computed the confidence interval of prediction between the mitochondrial counts and the library size with data from all 5,013,314 cells. We found that the relationship is noisy but positive and linear ($r = 0.65, P < 2.2 \times 10^{-16}$) as displayed in Fig. 1. Following this procedure, we identified 333,712 cells with mitochondrial counts above ($n = 178{,}671$) or below ($n = 155{,}041$) the computed confidence interval limits, which were also removed. After this step, 4,679,602 cells were retained for the study.

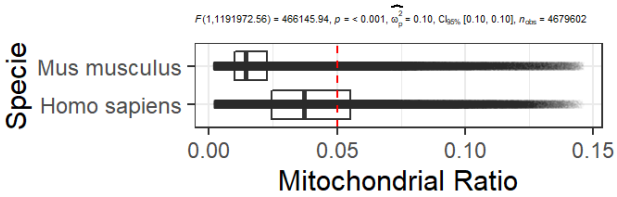

Fig 2. Boxplots showing the differences in the mtDNA% between human and mice cells. Each dot represents a cell; the red line is the early established 5% threshold.

With the cleaned dataset, we estimated that the mtDNA% per cell is distributed between the minimum of 0.17% and the maximum of 14.64%, considerably lower than the upper limit previously reported (up to 30% in heart) using the bulk RNA-seq generated by the Illumina Body Tissue Atlas (Mercer, Neph et al. 2011). Next, we performed a comparison to evaluate whether there is a difference in the average mtDNA% cross different species. The PanglaoDB database contains human and mouse datasets; therefore, our comparison was between human and mouse. We performed the Welch two-sample t-test and use the Wilcoxon-sum rank test to validate the results. Both tests converged to the same conclusion, that is, the average mtDNA% in human cells is significative higher than that in mice cells ($P < 2.2 \times 10^{-16}$, in both cases) as is displayed in Fig. 2.

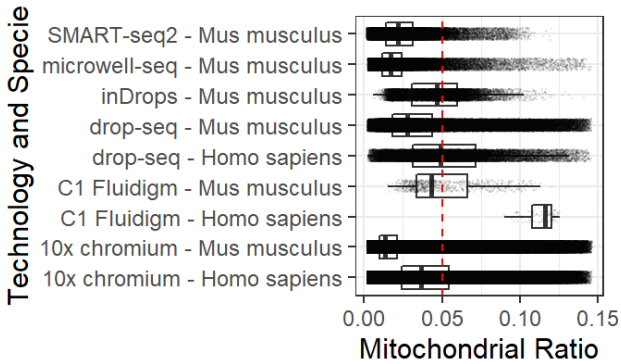

Fig 3. Boxplots showing the differences in the mtDNA% between human and mice cells by the technology used to generate the data. Each dot represents a cell; the red line is the early established 5% threshold.

Then, we compared the mitochondrial content between human and mouse data, stratified by the type of scRNA-seq technologies, by which the data is obtained. These technologies include drop-seq, C1 Fluidigm and 10x Genomics. Our results confirm our previous finding. In all cases wherever data allowed, no matter which technology is used, the same pattern was recovered. That is, Human cells have significantly larger mtDNA% than mice cells (Fig. 3). Most importantly, for all cases where mitochondrial content in humans were evaluated, the 75th percentile was located above the threshold, suggesting that the early defined 5% is not appropriate for human cells.

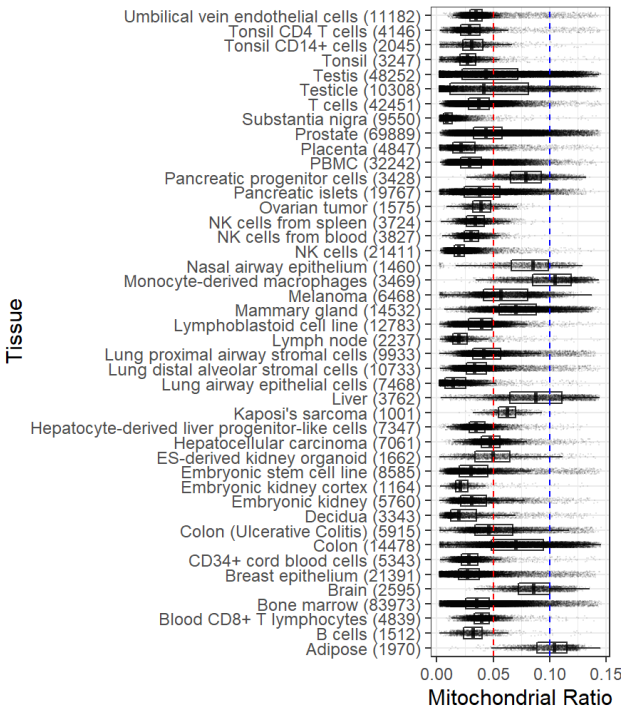

Fig 4. Boxplots of the mtDNA% across 44 human tissues. In parenthesis, the number of cells in the stated tissue. Each dot represents a cell, the red line is the stablished 5% threshold, blue line is the 10% threshold for human cells proposed here.

Note that 91.3% ($n = 4{,}271{,}613$) of cells analyzed here were processed using the 10x Genomics chromium system. Next, we decided to

perform the comparison of the mitochondrial content between tissues and cell types using only the data generated using the 10x Genomics technology.

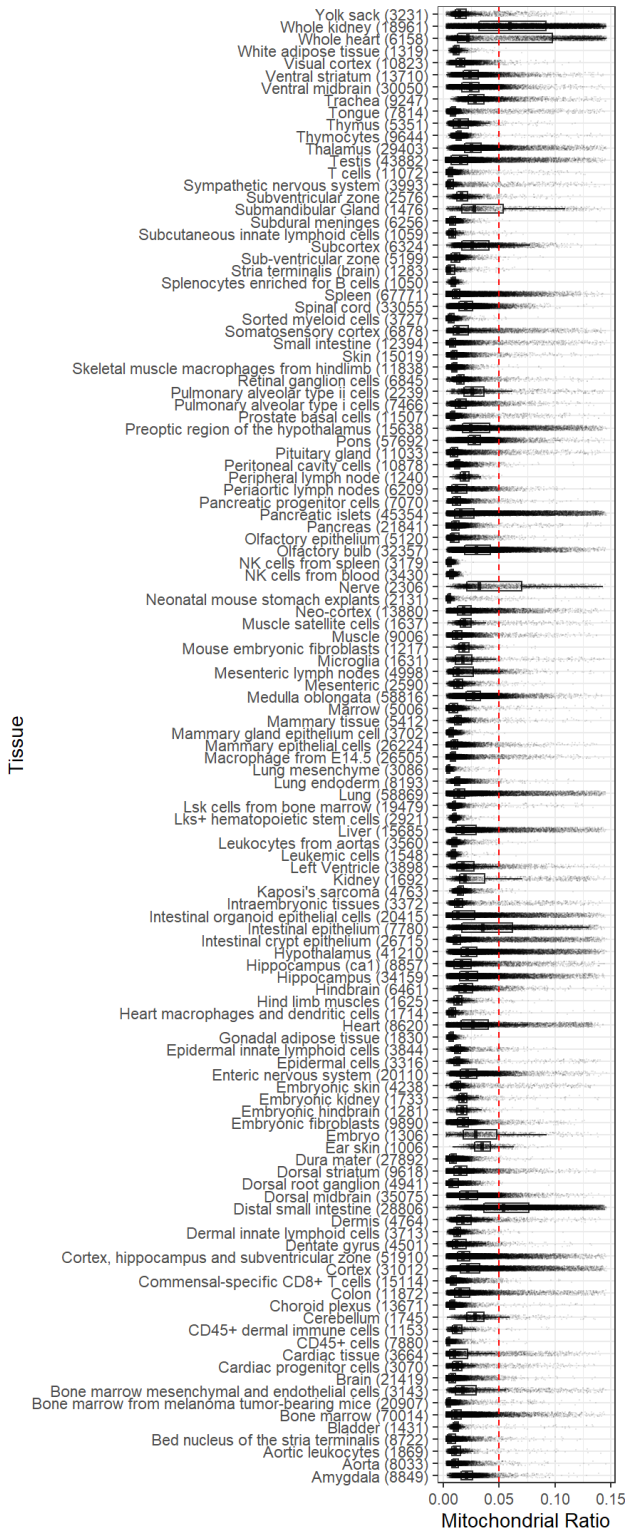

Fig 5. Boxplots of the mtDNA% across 121 mouse tissues. In parenthesis, the number of cells in the stated tissue. Each dot represents a cell, the red line is the stablished 5% threshold.

For human, we identified 44 tissues, for which more than 1,000 cells are available in the database. From those 44 tissues, 13 (29.5%) showed an average mtDNA% significantly higher than 5%. The 13 human tissues are nasal airway epithelium, monocyte-derived macrophages, testicle, colon (ulcerative colitis), liver, colon, melanoma, mammary gland, ES-derived kidney organoid, pancreatic progenitor cells, adipose, Kaposi's sarcoma, and brain. However, as displayed in Fig. 4, 18 of the 44 human tissues (40%) have a portion of the interquartile range over the 5% threshold. Only two of them, monocyte-derived macrophages and adipose, have an average mtDNA% higher than 10%. This result supports our observation that the early defined 5% is not appropriate for human tissues. We conclude that the new standardized threshold for human tissues should be 10% instead. At the cell-type level, we found similar patterns. From 37 different cell types with more than 1,000 cells derived from human samples, 13 of them (35.1%) have an average mtDNA% greater than 5% but none of them have an average mtDNA% greater than 10% (Fig. S2). The 13 cell types are hepatocytes, epithelial cells, neutrophils, cholangiocytes, smooth muscle cells, keratinocytes, Langerhans cells, spermatocytes, ductal cells, beta cells, luminal epithelial cells, macrophages, and embryonic stem cells. Furthermore, only 4 of them (epithelial cells, Langerhans cells, spermatocytes and macrophages) have a portion of the interquartile range above the 10% threshold.

For mice, when the mtDNA% was compared across the cell types with at least 1000 cells reported in the database, 7 of 74 cell types showed an average mtDNA% greater than 5%. The 7 cell types are proximal tubule cells, distal tubule cells, hepatocyte, cardiomyocytes, Leydig cells, intercalated cells, choroid plexus cell (Fig S3). In contrast to the identified 44 human tissues, there are much more mouse tissues (121) with more than 1,000 cells reported in the database. Among them, only 3 (2.5%) showed an average mtDNA% significative higher than 5% (whole kidney, whole heart, and distal small intestine). Furthermore, only 6 mouse tissues (Whole kidney, Intestinal epithelium, Whole heart, Nerve, Distal small intestine, and Submandibular Gland) have a portion of the interquartile range over the 5% threshold (Fig. 5). These findings indicate that the 5% threshold early proposed in the field is an appropriate standardized threshold for mouse tissues.

In summary, we reported updated reference mitochondrial proportion values across human and mice tissues and cell-types for scRNA-seq QC. Based on the results, we suggest a standardized mtDNA% threshold of 10% for scRNA-seq QC of human samples. For mouse samples, we found that the early defined 5% threshold accurately discriminates between healthy and apoptotic cells. Based on this evidence, we suggest that all published mouse studies, in which scRNA-seq QC was based on the mtDNA% value greater than 5%, should be re-evaluated. Because the use of a higher than 5% mtDNA% threshold may introduce possible biases in the data analysis.

Acknowledgements

We thank Dr. Chapkin lab members from the Texas A&M nutrition department for their thoughtful questions that motivated this paper.

Funding

This work has been supported by Texas A&M University X-grant for J.C.

Conflict of Interest: none declared.

References

AlJanahi AA, Danielsen M, Dunbar CE. 2018. An Introduction to the Analysis of Single-Cell RNA-Sequencing Data. *Mol Ther Methods Clin Dev* **10**: 189-196.

Franzen O, Gan LM, Bjorkegren JLM. 2019. PanglaoDB: a web server for exploration of mouse and human single-cell RNA sequencing data. *Database (Oxford)* **2019**.

Guantes R, Rastrojo A, Neves R, Lima A, Aguado B, Iborra FJ. 2015. Global variability in gene expression and alternative splicing is modulated by mitochondrial content. *Genome Res* **25**: 633-644.

Hwang B, Lee JH, Bang D. 2018. Single-cell RNA sequencing technologies and bioinformatics pipelines. *Exp Mol Med* **50**: 96.

Ilicic T, Kim JK, Kolodziejczyk AA, Bagger FO, McCarthy DJ, Marioni JC, Teichmann SA. 2016. Classification of low quality cells from single-cell RNA-seq data. *Genome Biol* **17**: 29.

Ji F, Sadreyev RI. 2019. Single-Cell RNA-seq: Introduction to Bioinformatics Analysis. *Curr Protoc Mol Biol* **127**: e92.

Lang DT, CRAN Team. 2012. XML: Tools for parsing and generating XML within R and S-Plus. 3.9-4.1.

Luecken MD, Theis FJ. 2019. Current best practices in single-cell RNA-seq analysis: a tutorial. *Mol Syst Biol* **15**: e8746.

Lukassen S, Bosch E, Ekici AB, Winterpacht A. 2018. Single-cell RNA sequencing of adult mouse testes. *Sci Data* **5**: 180192.

Lun AT, McCarthy DJ, Marioni JC. 2016. A step-by-step workflow for low-level analysis of single-cell RNA-seq data with Bioconductor. *F1000Res* **5**: 2122.

Ma A, Zhu Z, Ye M, Wang F. 2019. EnsembleKQC: An Unsupervised Ensemble Learning Method for Quality Control of Single Cell RNA-seq Sequencing Data. In *International Conference on Intelligent Computing*, pp. 493-504. Springer.

McCarthy DJ, Campbell KR, Lun AT, Wills QF. 2017. Scater: pre-processing, quality control, normalization and visualization of single-cell RNA-seq data in R. *Bioinformatics* **33**: 1179-1186.

Mercer TR, Neph S, Dinger ME, Crawford J, Smith MA, Shearwood AM, Haugen E, Bracken CP, Rackham O, Stamatoyannopoulos JA et al. 2011. The human mitochondrial transcriptome. *Cell* **146**: 645-658.

Muir R, Diot A, Poulton J. 2016. Mitochondrial content is central to nuclear gene expression: Profound implications for human health. *Bioessays* **38**: 150-156.

Ordonez-Rueda D, Baying B, Pavlinic D, Alessandri L, Yeboah Y, Landry JJM, Calogero R, Benes V, Paulsen M. 2020. Apoptotic Cell Exclusion and Bias-Free Single-Cell Selection Are Important Quality Control Requirements for Successful Single-Cell Sequencing Applications. *Cytometry A* **97**: 156-167.

R Core Team. 2013. R: A language and environment for statistical computing.

Sandberg R. 2014. Entering the era of single-cell transcriptomics in biology and medicine. *Nat Methods* **11**: 22-24.

Satija R, Farrell JA, Gennert D, Schier AF, Regev A. 2015. Spatial reconstruction of single-cell gene expression data. *Nat Biotechnol* **33**: 495-502.

Svensson V, da Veiga Beltrame E, Pachter L. 2019. A curated database reveals trends in single-cell transcriptomics. *bioRxiv*.

Wickham H, Hester J, Ooms J. 2018. xml2: Parse XML. R Package Version 1.2. 0.

Zhao Q, Wang J, Levichkin IV, Stasinopoulos S, Ryan MT, Hoogenraad NJ. 2002. A mitochondrial specific stress response in mammalian cells. *EMBO J* **21**: 4411-4419.

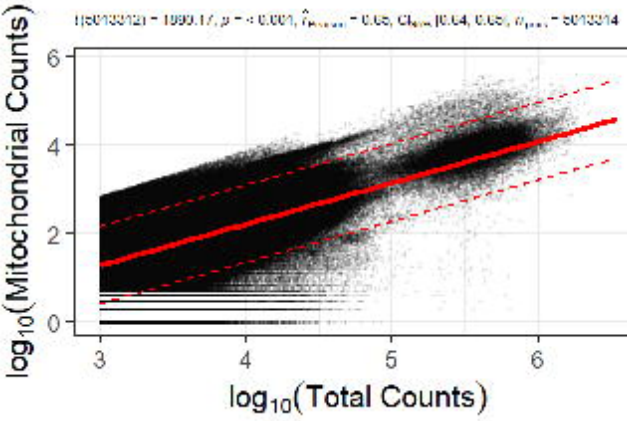
log10(Mitochondrial Counts)
log10(Total Counts)
0
2
4
6
3
4
5
6

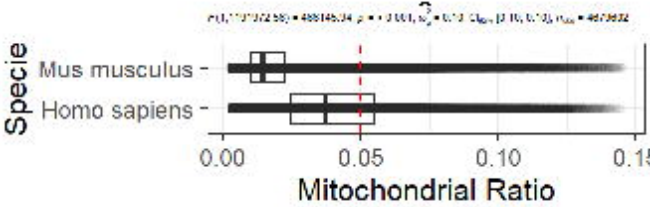
Specie
Mus musculus
Homo sapiens
0.00
0.05
0.10
0.15
Mitochondrial Ratio

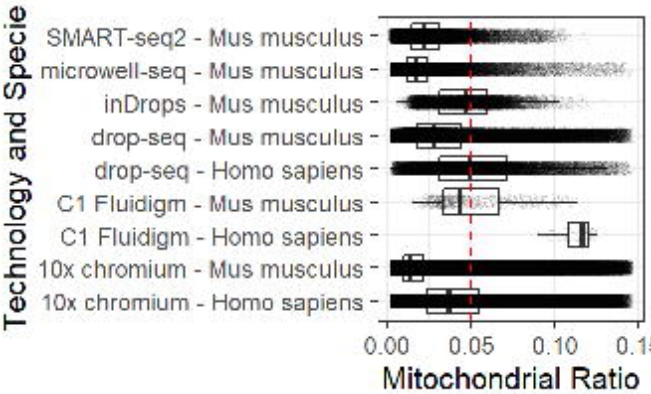
Technology and Specie
SMART-seq2 - Mus musculus
microwell-seq - Mus musculus
inDrops - Mus musculus
drop-seq - Mus musculus
drop-seq - Homo sapiens
C1 Fluidigm - Mus musculus
C1 Fluidigm - Homo sapiens
10x chromium - Mus musculus
10x chromium - Homo sapiens
0.00
0.05
0.10
0.15
Mitochondrial Ratio

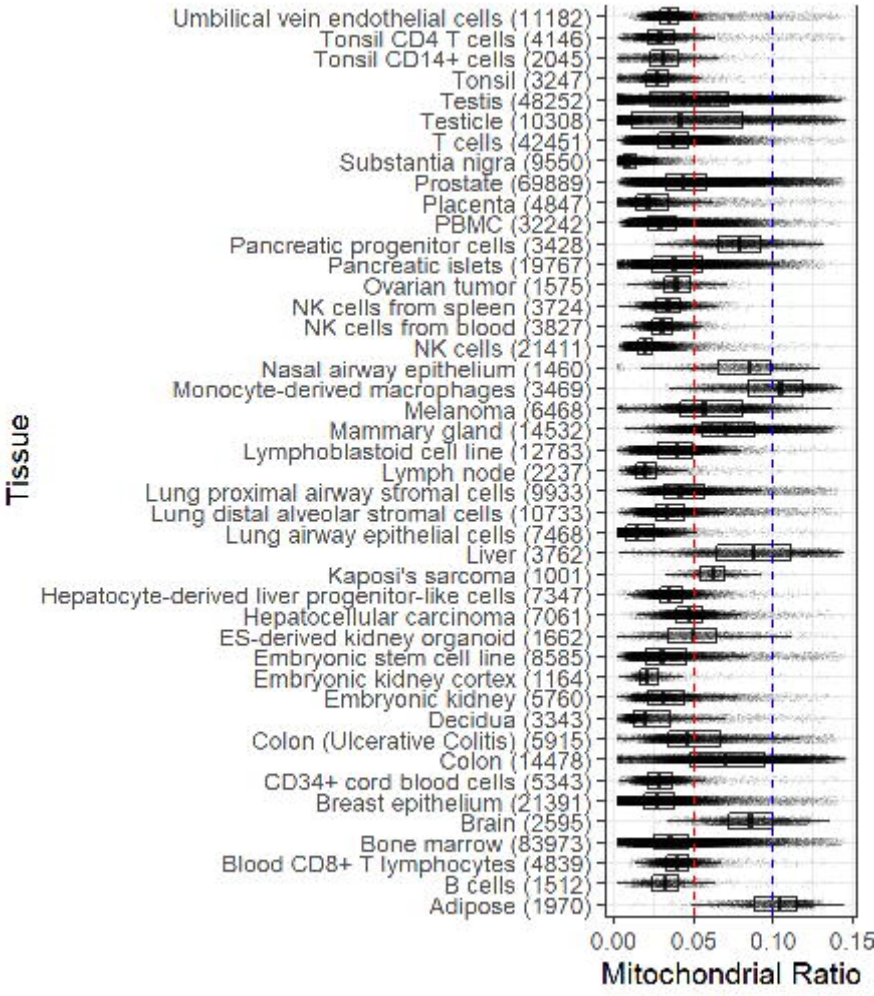
Umbilical vein endothelial cells (11182)
Tonsil CD4 T cells (4146)
Tonsil CD14+ cells (2045)
Tonsil (3247)
Testis (48252)
Testicle (10308)
T cells (42451)
Substantia nigra (9550)
Prostate (69889)
Placenta (4847)
PBMC (32242)
Pancreatic progenitor cells (3428)
Pancreatic islets (19767)
Ovarian tumor (1575)
NK cells from spleen (3724)
NK cells from blood (3827)
NK cells (21411)
Nasal airway epithelium (1460)
Monocyte-derived macrophages (3469)
Melanoma (6468)
Mammary gland (14532)
Lymphoblastoid cell line (12783)
Lymph node (2237)
Lung proximal airway stromal cells (9933)
Lung distal alveolar stromal cells (10733)
Lung airway epithelial cells (7468)
Liver (3762)
Kaposi's sarcoma (1001)
Hepatocyte-derived liver progenitor-like cells (7347)
Hepatocellular carcinoma (7061)
ES-derived kidney organoid (1662)
Embryonic stem cell line (8585)
Embryonic kidney cortex (1164)
Embryonic kidney (5760)
Decidua (3343)
Colon (Ulcerative Colitis) (5915)
Colon (14478)
CD34+ cord blood cells (5343)
Breast epithelium (21391)
Brain (2595)
Bone marrow (83973)
Blood CD8+ T lymphocytes (4839)
B cells (1512)
Adipose (1970)
Tissue
0.00
0.05
0.10
0.15
Mitochondrial Ratio

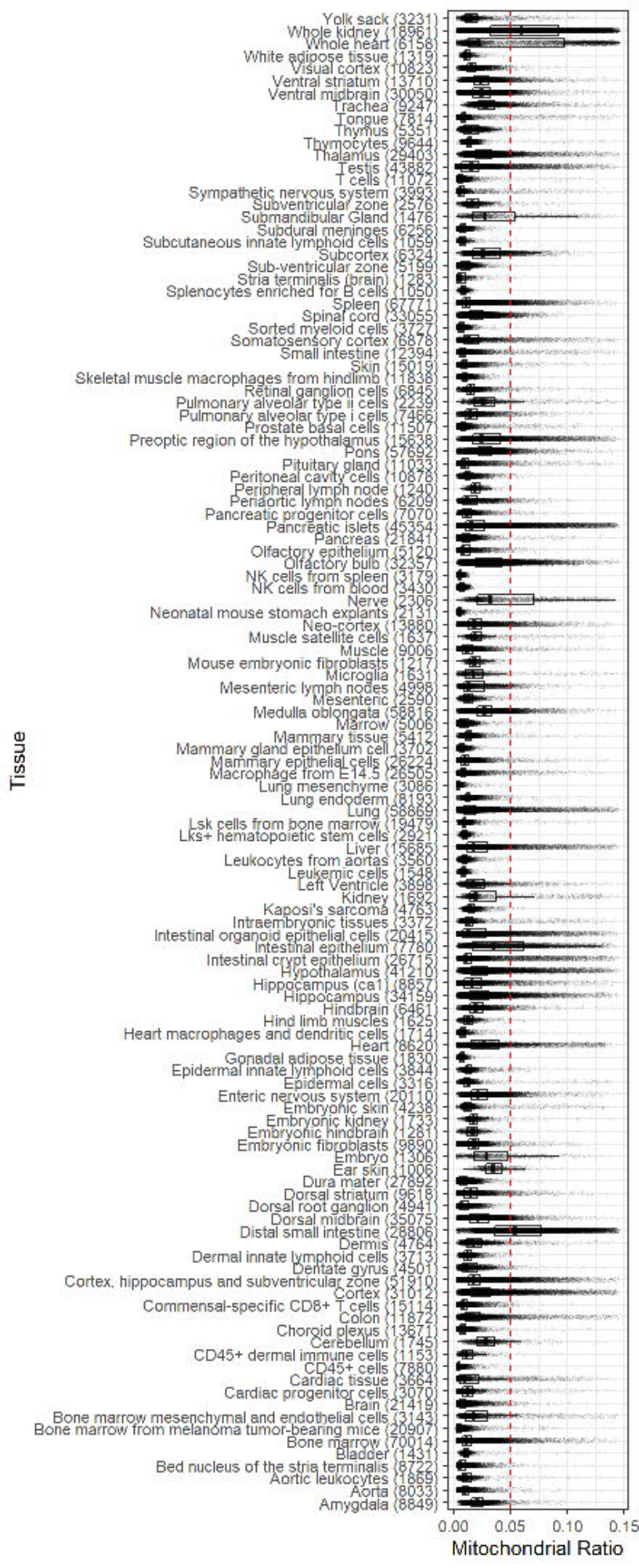
Yolk sack (3231)
Whole kidney (18961)
Whole heart (6158)
White adipose tissue (1319)
Visual cortex (10823)
Ventral striatum (13710)
Ventral midbrain (30050)
Trachea (9247)
Tongue (7814)
Thymus (5351)
Thymocytes (9644)
Thalamus (29403)
Testis (43882)
T cells (11072)
Sympathetic nervous system (3993)
Subventricular zone (2576)
Submandibular Gland (1476)
Subdural meninges (6258)
Subcutaneous innate lymphoid cells (1059)
Subcortex (6324)
Sub-ventricular zone (5199)
Stria terminalis (brain) (1283)
Splenocytes enriched for B cells (1050)
Spleen (67771)
Spinal cord (33055)
Sorted myeloid cells (3727)
Somatosensory cortex (6876)
Small intestine (12394)
Skin (15019)
Skeletal muscle macrophages from hindlimb (11838)
Retinal ganglion cells (6845)
Pulmonary alveolar type ii cells (2239)
Pulmonary alveolar type i cells (7466)
Prostate basal cells (11507)
Preoptic region of the hypothalamus (15638)
Pons (57692)
Pituitary gland (11033)
Peritoneal cavity cells (10878)
Peripheral lymph node (1240)
Periaortic lymph nodes (6209)
Pancreatic progenitor cells (7070)
Pancreatic islets (45354)
Pancreas (21841)
Olfactory epithelium (5120)
Olfactory bulb (32357)
NK cells from spleen (3179)
NK cells from blood (3430)
Nerve (2306)
Neonatal mouse stomach explants (2131)
Neo-cortex (13880)
Muscle satellite cells (1637)
Muscle (9006)
Mouse embryonic fibroblasts (1217)
Microglia (1631)
Mesenteric lymph nodes (4998)
Mesenteric (2590)
Medulla oblongata (58816)
Marrow (5006)
Mammary tissue (5412)
Mammary gland epithelium cell (3702)
Mammary epithelial cells (26224)
Macrophage from E14.5 (26505)
Lung mesenchyme (3086)
Lung endoderm (8193)
Lung (58869)
Lsk cells from bone marrow (19479)
Lks+ hematopoietic stem cells (2921)
Liver (15685)
Leukocytes from aortas (3560)
Leukemic cells (1548)
Left Ventricle (3898)
Kidney (1692)
Kaposi's sarcoma (4763)
Intraembryonic tissues (3372)
Intestinal organoid epithelial cells (20415)
Intestinal epithelium (7780)
Intestinal crypt epithelium (26715)
Hypothalamus (41210)
Hippocampus (ca1) (8857)
Hippocampus (34159)
Hindbrain (6461)
Hind limb muscles (1625)
Heart macrophages and dendritic cells (1714)
Heart (8620)
Gonadal adipose tissue (1830)
Epidermal innate lymphoid cells (3844)
Epidermal cells (3316)
Enteric nervous system (20110)
Embryonic skin (4238)
Embryonic kidney (1733)
Embryonic hindbrain (1281)
Embryonic fibroblasts (9890)
Embryo (1306)
Ear skin (1006)
Dura mater (27892)
Dorsal striatum (9618)
Dorsal root ganglion (4941)
Dorsal midbrain (35075)
Distal small intestine (28806)
Dermis (4764)
Dermal innate lymphoid cells (3713)
Dentate gyrus (4501)
Cortex, hippocampus and subventricular zone (51910)
Cortex (31012)
Commensal-specific CD8+ T cells (15114)
Colon (11872)
Choroid plexus (13671)
Cerebellum (1745)
CD45+ dermal immune cells (1153)
CD45+ cells (7880)
Cardiac tissue (3664)
Cardiac progenitor cells (3070)
Brain (21419)
Bone marrow mesenchymal and endothelial cells (3143)
Bone marrow from melanoma tumor-bearing mice (20907)
Bone marrow (70014)
Bladder (1431)
Bed nucleus of the stria terminalis (8722)
Aortic leukocytes (1869)
Aorta (8033)
Amygdala (8849)
Tissue
0.00
0.05
0.10
0.15
Mitochondrial Ratio